Numerical analysis of the Bivariate Local Linearization Method (BLLM) for partial differential equations in Casson fluid flow

GILBERT MAKANDA
Central University
of
Technology
Department of Mathematical and Physical Sciences
Private Bag X20539, 9300 Bloemfontein
SOUTH AFRICA
gilbertmakanda@yahoo.com

SACHIN SHAW
Botswana International University
of
Science and Technology
Department of Mathematics and Statistical Sciences
Private Bag 6,Palapye
BOTSWANA
sachinshaw@gmail.com

Abstract: The double diffusion convection Casson fluid flow along a vertical plate incorporating Soret effect and viscous heating with thermal and solutal dispersion was studied. A well-known system of non-similar partial differential equations was solved using the bivariate local linearization method (BLLM). The solution procedure uses an approximation by a bivariate Lagrange interpolation polynomial. Older methods considered collocations along the non-dimensional boundary layer axis η only. In this paper collocations in both the (η, ζ) directions are considered. The numerical method is compared to the results obtained by the quasi-linearization method (QLM) and those previously published in the literature for the case $(\zeta = 0)$. This work also analyse the efficiency and robustness of the numerical method used as compared to traditional methods such as finite differences widely used in the literature. The increase in thermal stratification parameter decrease heat transfer coefficient and increase mass transfer coefficient. The increase in the non-Newtonian parameter result in the increase velocity profiles, skin friction coefficient and reduce both temperature and concentration profiles. Increasing the Biot number decrease temperature trends.

Key–Words: Soret effect, Casson, dispersion, viscous heating, BLLM

1 Introduction

The study of the double dispersion in convection and fluid flow in a double stratified medium has become popular due to its environmental and engineering applications. Applications include dispersion of chemical wastes in ground water flow and other forms of pollution, liquification and grain storage. Other applications arise in products in pharmacy, the reaction of coal and water, flow of paints and lubricants [1] - [2]. Fluid flow involving mechanical dispersion in Casson fluid, the movement of iron fillings in engine oil, the solute transfer in human blood and the distribution of solutal objects in soups has received little attention.

Dispersion in fluid flow is the mechanical movement of solute due to a concentration gradient in the flow regime. The study of the concept of dispersion was done by among others Narayana and Murthy [3] who studied the transfer of heat and mass in a double stratified medium with non-Darcy porous conditions. Kairi and Murthy [4] investigated natural convection in a non-Darcy porous thermally stratified medium. These studies advanced the understanding of dispersion and thermal stratification. The effect of the double dispersion in micropolar fluid has been studied by Srinivasacharya and RamReddy [5]. Murthy et al. [6] investigated the effect of fluid flow in nanofluid saturated non-Darcy porous medium with thermal stratification. Kameswaran and Sibanda [7] studied the fluid flow in heat, mass transfer and convection in a porous media of Ostwald de Waele nanofluid flow with thermal dispersion.

Studies on vertical plate geometry include the work of Chen [8] which focused on vertical surface, MHD and Ohmic heating. Narayana et al.[9] worked on vertical wavy surface, Soret and Dufour effects. Javaherdehdeh [10] investigated fluid flow on a vertical surface, heat and mass transfer in porous media. Raju et al. [11] worked on viscous dissipation and magnetic effects on the flow of fluid along a vertical plate.

The study of shear thinning Casson fluid flow has attracted attention due to its industrial application and biological fluids such as blood and synovial fluid. Casson fluid is a non- Newtonian fluid that show unique shear-stress-strain relationships and these are different from Newtonian fluids. The non-linear constitutive equation for Casson fluid was derived by Casson [12] in 1959. It describes a wide range of shear rates for properties of many polymers (Vinogradov and Malkin [13]). The Casson fluid model describes blood flowing through small vessels with low shear rate (McDonald [14]; Shaw et al. [15]). Studies in non-Newtonian fluids such as Casson fluid

flow include among others the work of Mukhopaddhyay et. al [16] who worked on the flow of Casson fluid along a stretching surface, Mukhopadhyay and Vajravelu [17] studied Casson fluid flow along a porous stretching surface with diffusion and chemical reaction species. Nadeem et. al [18] investigated magneto-hydrodynamic three-dimensional Casson fluid flow on a linearly stretching surface. All of these studies improved the understanding of Casson fluid behaviour.

In all the studies mentioned above, viscous heating was not considered. Viscous heating effects on Newtonian fluid flow were considered by among others Jordan [19] who studied the effects of viscous heating on unsteady natural convection over vertical porous plate. The influence of viscous heating on a grey emitting/absorbing fluid flow along a moving vertical plate has been studied by Suneetha et al. [20]. Kameswaran et al. [21] studied the effect of viscous heating on magneto-hydrodynamic nanofluid flow due to a shrinking/stretching sheet. These studies emphasized the importance of considering heat generated by fluid flow. In this paper, viscous dissipation in Casson fluid flow is considered.

Motivated by all of the above studies, the aim of this work is to study double dispersion in Casson fluid flow along vertical plate with consideration of Soret and viscous heating effects. The governing equations were solved numerically using the bivariate local linearization method which is in [23]. The general systematic way of presenting the local linearization and quasi-linearization methods is shown for brevity. This gives the general approach that can be used in solving partial differential equations. The influence of the different parameters on concentration, temperature and velocity profiles is discussed through graphical illustrations. The effect of Casson parameter, solutal convection parameter, double diffusion parameter, stratification parameter and the Biot number are considered in this study. The effect of radiation, Prandtl and Schmidt numbers on the fluid properties is not discussed as they are well known.

2 Mathematical formulation

In this paper we consider a steady, two dimensional Casson fluid flow adjacent to a vertical surface. The x-coordinate is along the vertical plate and y is normal to the surface of the plate, u and v are the velocity components in the directions of x and y respectively. The vertical plate surface is maintained at constant temperature T_w and concentration on the vertical plate is C_w. A model of an incompressible as well as isotropic flow of Casson fluid is written as

$$t_{ij} = \left(\mu_e^{\frac{1}{n}} + (t_y/\sqrt{2\pi})^{\frac{1}{n}}\right)^n e_{ij}, \quad |t_{ij}| > t_y$$
$$\text{if } |t_{ij}| < t_y \text{ then } \pi = 0, \text{ there is no flow.} \quad (1)$$

where t_y is the yield stress of the Casson fluid, $\pi = e_{ij}e_{ij}$, e_{ij} is the (i,j)-th component of the rate of deformation, μ_e is plastic dynamic viscosity of the Casson fluid, For $n = 2$ represents the simple model for Casson fluid. In this paper we use the value $n = 1$ as used in [2],[16],[17] and [18].

Considering the effect of the thermal and solutal dispersion, the double dispersion convection equation of the Casson fluid is written as

$$\frac{\partial u}{\partial x} + \frac{\partial v}{\partial y} = 0, \quad (2)$$

$$u\frac{\partial u}{\partial x} + v\frac{\partial u}{\partial y} = \nu\left(1 + \frac{1}{\delta}\right)\frac{\partial^2 u}{\partial y^2} \pm g\beta_T(T - T_\infty) + g\beta_c(C - C_\infty), \quad (3)$$

$$u\frac{\partial T}{\partial x} + v\frac{\partial T}{\partial y} = \frac{\partial}{\partial y}\left(\alpha_y\frac{\partial T}{\partial y}\right) - \frac{1}{\rho C_p}\frac{\partial q_r}{\partial y} + \frac{\nu}{Cp}\left(1 + \frac{1}{\delta}\right)\left(\frac{\partial u}{\partial y}\right)^2, \quad (4)$$

$$u\frac{\partial C}{\partial x} + v\frac{\partial C}{\partial y} = \frac{\partial}{\partial y}\left(D_y\frac{\partial C}{\partial y}\right) + \frac{D_T}{T_m}\frac{\partial^2 T}{\partial y^2}, \quad (5)$$

and the boundary conditions are written as

$$\left.\begin{aligned} &u = v = 0,\ k_f\frac{\partial T}{\partial y} = h_0(T_0 - T), \\ &C = C_w, \text{ at } y = 0, \\ &u \to U,\ T \to T_\infty,\ C \to C_\infty, \text{ as } y \to \infty. \end{aligned}\right\} \quad (6)$$

where ν is the viscosity of the fluid, g is the gravitational acceleration, $\delta = \mu\sqrt{2\pi_c}/\tau_y$ is the Casson parameter, β_T and β_C are the thermal and solutal coefficients of expansions respectively, T is the solute temperature, T_∞ is uniform ambient temperature, C is the solute concentration, C_∞ is uniform ambient concentration, $\alpha_y = \alpha + \gamma d(\partial\psi/\partial y)$ and $D_y = D_{sm} + \xi d(\partial\psi/\partial y)$ represent the thermal dispersion and solutal diffusivity, respectively where α is the molecular thermal diffusivity, γ is the mechanical thermal-dispersion coefficient, D_{sm} is the solutal diffusivity and ξ is the mechanical solutal-dispersion coefficient, D_T is the thermal diffusivity,q_r is the radiative heat flux, C_p is the specific heat capacity, T_m is the mean fluid temperature. The convective boundary conditions at the surface are considered, the surface is heated by fluid of temperature T_0 and provide a heat transfer coefficient h_0 and thermal conductivity k_0 where $T_0 > T_w > T_\infty$. The approximation for the Roseland radiation is;

$$q_r = -\frac{4\sigma}{3k^*}\frac{\partial T^4}{\partial y} \quad (7)$$

where k^* and σ are the absorption and Stefan-Boltzmann numbers, the temperature gradient within the fluid flow is given by T^4 and the Taylor series expansion about T_∞ and discarding higher powers we

have $T^4 - 4T_\infty^3 - 3T_\infty^4$ and therefore (4) can be presented as

$$u\frac{\partial T}{\partial x} + v\frac{\partial T}{\partial y} = \frac{\partial}{\partial y}\left(\alpha_y \frac{\partial T}{\partial y}\right) - \frac{16\sigma T_\infty^2}{3\nu C_p k^*}\frac{\partial^2 T}{\partial y^2} + \frac{\nu}{Cp}\left(1+\frac{1}{\delta}\right)\left(\frac{\partial u}{\partial y}\right)^2 \quad (8)$$

Using the following transformations

$$\left.\begin{aligned} \zeta = \frac{x}{l},\ \eta = \sqrt{\frac{U}{\nu x}}y,\ \theta = \frac{T-T_\infty}{T_f - T_\infty}, \\ \psi = \sqrt{\nu U x} f(\zeta,\ \eta),\ \phi = \frac{C - C_\infty}{C_w - C_\infty}. \end{aligned}\right\} \quad (9)$$

then the governing system of equations are obtained as follows

$$\left(1+\frac{1}{\delta}\right) f''' + \frac{1}{2} f f'' \pm \lambda\zeta(\theta + N\phi) = \zeta\left(f'\frac{\partial f'}{\partial \zeta} - f''\frac{\partial f}{\partial \zeta}\right), \quad (10)$$

$$\frac{1}{Pr}\left(1+\frac{4}{3}R\right)\theta'' + \frac{1}{2}f\theta' + \left(1+\frac{1}{\delta}\right)Ecf''^2 + \epsilon_1\left(f''\theta' + f'\theta''\right) = \zeta\left(f'\frac{\partial \theta}{\partial \zeta} - \theta'\frac{\partial f}{\partial \zeta}\right), \quad (11)$$

$$\frac{1}{Sc}\phi'' + \frac{1}{2}f\phi' + Sr\theta'' + \epsilon_2\left(f''\phi' + f'\phi''\right) = \zeta\left(f'\frac{\partial \phi}{\partial \zeta} - \phi'\frac{\partial f}{\partial \zeta}\right), \quad (12)$$

and the boundary conditions are written as

$$\left.\begin{aligned} f'(\zeta,0) = f(\zeta,0) + 2\zeta\frac{\partial f}{\partial \zeta}(\zeta,0) = 0, \\ \theta' = -Bi\left(1-\theta(\zeta,0)\right),\ \phi(\zeta,0) = 1, \\ f'(\zeta,\infty)\to 1,\ \theta(\zeta,\infty)\to 0, \\ \phi(\zeta,\infty)\to 0. \end{aligned}\right\} \quad (13)$$

where f' denotes the derivative with respect to η. Thermal Grashof number (Gr), Reynolds number (Re), Solute Grashof number (Gr^*), thermal convection parameter (λ), solutal convection parameter (λ^*), double diffusion parameter (N), thermal stratification parameter (ϵ_1), solutal stratification parameter (ϵ_2), radiation parameter (R), Eckert number (Ec), Soret number (Sr), Biot number (Bi) and Schmidt number (Sc), defined as

$$\left.\begin{aligned} Gr = \frac{g\beta_T \Delta T L^3}{\nu^2},\ Re = \frac{UL}{\nu}, \\ \epsilon_2 = \xi\frac{dU}{\nu}, \lambda = \frac{Gr}{Re^2}, \lambda^* = \frac{Gr^*}{Re^2} \\ Bi = \frac{a}{k_f}\sqrt{\frac{\nu}{U}},\ N = \frac{\lambda^*}{\lambda}, \\ \epsilon_1 = \gamma\frac{dU}{\nu},\ Gr^* = \frac{g\beta_c \Delta C L}{U^2}, \\ R = \frac{16T_\infty^2\sigma}{3\nu k^*},\ Ec = \frac{\nu U^2}{Cp\Delta T}, \\ Sc = \frac{\nu}{D},\ Sr = \frac{DK_T\Delta T}{\nu T_m \Delta C}, \end{aligned}\right\} \quad (14)$$

The important non-dimensional parameters are C_F (skin friction), Nu_X (local Nusselt number) and Sh_X (local Sherwood number) are written as

$$\left.\begin{aligned} Ra_X^{1/2}\, C_F = \left(1+\frac{1}{\delta}\right) f''(0), \\ Ra_X^{-1/2}\, Nu_X = -[1+\epsilon_1 f'(0)]\theta'(0), \\ Ra_X^{-1/2}\, Sh_X = -[1+\epsilon_2 f'(0)]\phi'(0), \end{aligned}\right\} \quad (15)$$

3 Method of solution

In this section the bivariate local linearization method (BLLM)is implemented, which is found in ([23]). The quasi-linearization method (QLM) is used and was first used by Bellman and Kalaba [24] to equations (10)-(12). Assuming that the differences $(f_{r+1} - f_r)$,$(\theta_{r+1} - \theta_r)$ and all its derivatives are small. In this section a systematic way of implementing the quasi-linearization and the local linearization methods is shown.

3.1 Quasi-linearization Method (QLM)

Partial differential equations can be solved using the quasi-linearization method which can be represented systematically by considering the following representation; Given the general partial differential equation of the form

$$\left.\begin{aligned} \Gamma_1\left[h_1, h_2, \ldots, h_n\right] = 0, \\ \Gamma_2\left[h_1, h_2, \ldots, h_n\right] = 0, \\ \vdots \\ \Gamma_n\left[h_1, h_2, \ldots, h_n\right] = 0, \end{aligned}\right\} \quad (16)$$

where

$$h_i = \left[f_1, \frac{\partial f_1}{\partial \eta}, \frac{\partial^2 f_1}{\partial \eta^2}, \ldots, \frac{\partial^p f_1}{\partial \eta^p}, \frac{\partial f_1}{\partial \zeta}, \frac{\partial f_1'}{\partial \zeta}\right] \quad \text{for } i = 1, 2, \ldots, n \quad (17)$$

The linearized system is given by

$$\sum_{s=0}^{p}\alpha_{1,s,r}^{(1)}f_{1,r+1}^{(s)}+\sum_{s=0}^{p}\alpha_{2,s,r}^{(1)}f_{2,r+1}^{(s)}+\cdots+\sum_{s=0}^{p}\alpha_{n,s,r}^{(1)}f_{n,r+1}^{(s)}+\sum_{v=0}^{p}\left[\beta_{v,r}^{(1)}\frac{\partial f_{v,r+1}}{\partial\zeta}+\gamma_{v,r}^{(1)}\frac{\partial f'_{v,r+1}}{\partial\zeta}\right]=R_1 \quad (18)$$

$$\sum_{s=0}^{p}\alpha_{1,s,r}^{(2)}f_{1,r+1}^{(s)}+\sum_{s=0}^{p}\alpha_{2,s,r}^{(2)}f_{2,r+1}^{(s)}+\cdots+\sum_{s=0}^{p}\alpha_{n,s,r}^{(2)}f_{n,r+1}^{(s)}+\sum_{v=0}^{p}\left[\beta_{v,r}^{(2)}\frac{\partial f_{v,r+1}}{\partial\zeta}+\gamma_{v,r}^{(2)}\frac{\partial f'_{v,r+1}}{\partial\zeta}\right]=R_2 \quad (19)$$

$$\vdots$$

$$\sum_{s=0}^{p}\alpha_{1,s,r}^{(n)}f_{1,r+1}^{(s)}+\sum_{s=0}^{p}\alpha_{2,s,r}^{(n)}f_{2,r+1}^{(s)}+\cdots+\sum_{s=0}^{p}\alpha_{n,s,r}^{(n)}f_{n,r+1}^{(s)}+\sum_{v=0}^{p}\left[\beta_{v,r}^{(n)}\frac{\partial f_{v,r+1}}{\partial\zeta}+\gamma_{v,r}^{(n)}\frac{\partial f'_{v,r+1}}{\partial\zeta}\right]=R_n \quad (20)$$

where

$$R_1=\sum_{s=0}^{p}\alpha_{1,s,r}^{(1)}f_{1,r}^{(s)}+\sum_{s=0}^{p}\alpha_{2,s,r}^{(1)}f_{2,r}^{(s)}+\cdots+\sum_{s=0}^{p}\alpha_{n,s,r}^{(1)}f_{n,r}^{(s)}+\sum_{v=0}^{p}\left[\beta_{v,r}^{(1)}\frac{\partial f_{v,r}}{\partial\zeta}+\gamma_{v,r}^{(1)}\frac{\partial f'_{v,r}}{\partial\zeta}\right]-\Gamma_1 \quad (21)$$

$$R_2=\sum_{s=0}^{p}\alpha_{1,s,r}^{(2)}f_{1,r}^{(s)}+\sum_{s=0}^{p}\alpha_{2,s,r}^{(2)}f_{2,r}^{(s)}+\cdots+\sum_{s=0}^{p}\alpha_{n,s,r}^{(2)}f_{n,r}^{(s)}+\sum_{v=0}^{p}\left[\beta_{v,r}^{(2)}\frac{\partial f_{v,r}}{\partial\zeta}+\gamma_{v,r}^{(2)}\frac{\partial f'_{v,r}}{\partial\zeta}\right]-\Gamma_2 \quad (22)$$

$$\vdots$$

$$R_n=\sum_{s=0}^{p}\alpha_{1,s,r}^{(n)}f_{1,r}^{(s)}+\sum_{s=0}^{p}\alpha_{2,s,r}^{(n)}f_{2,r}^{(s)}+\cdots+\sum_{s=0}^{p}\alpha_{n,s,r}^{(n)}f_{n,r}^{(s)}+\sum_{v=0}^{p}\left[\beta_{v,r}^{(n)}\frac{\partial f_{v,r}}{\partial\zeta}+\gamma_{v,r}^{(n)}\frac{\partial f'_{v,r}}{\partial\zeta}\right]-\Gamma_n \quad (23)$$

Applying the systematic quasi-linearization method to (10)-(12) we rearrange as follows

$$\Gamma_1=\left(1+\frac{1}{\delta}\right)f'''+\frac{1}{2}ff''\pm\lambda\zeta(\theta+N\phi)-\zeta\left(f'\frac{\partial f'}{\partial\xi}-f''\frac{\partial f}{\partial\zeta}\right), \quad (24)$$

$$\Gamma_2=\frac{1}{Pr}\left(1+\frac{4}{3}R\right)\theta''+\frac{1}{2}f\theta'+\left(1+\frac{1}{\delta}\right)Ecf''^2+\epsilon_1\left(f''\theta'+f'\theta''\right)-\zeta\left(f'\frac{\partial\theta}{\partial\zeta}-\theta'\frac{\partial f}{\partial\zeta}\right), \quad (25)$$

$$\Gamma_3=\frac{1}{Sc}\phi''+\frac{1}{2}f\phi'+Sr\theta''+\epsilon_2\left(f''\phi'+f'\phi''\right)-\zeta\left(f'\frac{\partial\phi}{\partial\zeta}-\phi'\frac{\partial f}{\partial\zeta}\right), \quad (26)$$

By assigning $f_1=f, f_2=\theta, f_3=\phi$, we have the following linearized system

$$\alpha_{1,0,r}^{(1)}f_{1,r+1}+\alpha_{1,1,r}^{(1)}f'_{1,r+1}+\alpha_{1,2,r}^{(1)}f''_{1,r+1}+\alpha_{1,3,r}^{(1)}f'''_{1,r+1}+\alpha_{2,0,r}^{(1)}f_{2,r+1}+\alpha_{3,0,r}^{(1)}f_{3,r+1}+\beta_{0,r}^{(1)}\frac{\partial f_{1,r+1}}{\partial\zeta}+\gamma_{1,r}^{(1)}\frac{\partial f'_{1,r+1}}{\partial\zeta}=R_1, \quad (27)$$

$$\alpha_{2,0,r}^{(2)}f_{2,r+1}+\alpha_{2,1,r}^{(2)}f'_{2,r+1}+\alpha_{2,2,r}^{(2)}f''_{2,r+1}+\beta_{0,r}^{(2)}\frac{\partial f_{2,r+1}}{\partial\zeta}=R_2, \quad (28)$$

$$\alpha_{3,0,r}^{(3)}f_{3,r+1}+\alpha_{3,1,r}^{(3)}(\zeta,\eta)f'_{3,r+1}+\alpha_{3,2,r}^{(3)}f''_{3,r+1}+\beta_{0,r}^{(3)}\frac{\partial f_{3,r+1}}{\partial\zeta}=R_3. \quad (29)$$

where

$$\alpha^{(1)}_{1,0,r} = \frac{1}{2}f''_r,\ \alpha^{(1)}_{1,1,r} = -\zeta\frac{\partial f'_r}{\partial\zeta},$$
$$\alpha^{(1)}_{1,2,r} = \frac{1}{2}f_r + \zeta\frac{\partial f_r}{\partial\zeta},\ \alpha^{(1)}_{1,3,r} = \left(1+\frac{1}{\delta}\right),$$
$$\alpha^{(1)}_{2,0,r} = \lambda\zeta,\ \alpha^{(1)}_{3,0,r} = \lambda\zeta N,$$
$$\beta^{(1)}_{0,r} = \zeta f''_r,\ \gamma^{(1)}_{1,r} = -\zeta f'_r,$$
$$\begin{aligned} R_1 = {} & \alpha^{(1)}_{1,0,r}f_{1,r} + \alpha^{(1)}_{1,1,r}f'_{1,r} + \alpha^{(1)}_{1,2,r}f''_{1,r} \\ & + \alpha^{(1)}_{1,3,r}f'''_{1,r} + \alpha^{(1)}_{2,0,r}f_{2,r} + \alpha^{(1)}_{3,0,r}f_{3,r} \\ & + \beta^{(1)}_{0,r}\frac{\partial f_{1,r}}{\partial\zeta} + \gamma^{(1)}_{1,r}\frac{\partial f'_{1,r}}{\partial\zeta} - \Gamma_1, \end{aligned}$$

$$\alpha^{(2)}_{2,0,r} = 0,\ \alpha^{(2)}_{2,1,r} = \frac{1}{2}f_r + \zeta\frac{\partial f_r}{\partial\zeta} + \epsilon_1 f''_r,$$
$$\alpha^{(2)}_{2,2,r} = \frac{1}{Pr}\left(1+\frac{4}{3}R\right) + \epsilon_1 f'_r,\ \beta^{(2)}_{0,r} = -\zeta f'_r,$$
$$\begin{aligned} R_2 = {} & \alpha^{(2)}_{2,0,r}f_{2,r} + \alpha^{(2)}_{2,1,r}f'_{2,r} + \alpha^{(2)}_{2,2,r}f''_{2,r} \\ & + \beta^{(2)}_{0,r}\frac{\partial f_{2,r}}{\partial\xi} - \Gamma_2, \end{aligned}$$

$$\alpha^{(3)}_{3,0,r} = 0,\ \alpha^{(3)}_{3,1,r} = \frac{1}{2}f_r + \zeta\frac{\partial f_r}{\partial\zeta} + \epsilon_2 f''_r,$$
$$\alpha^{(3)}_{3,2,r} = \frac{1}{Sc} + \epsilon_2 f'_r,\ \beta^{(3)}_{0,r} = -\zeta f'_r$$
$$\begin{aligned} R_3 = {} & \alpha^{(3)}_{3,0,r}f_{3,r} + \alpha^{(3)}_{3,1,r}f'_{3,r} + \alpha^{(3)}_{3,2,r}f''_{3,r} \\ & + \beta^{(3)}_{0,r}\frac{\partial f_{3,r}}{\partial\zeta} - \Gamma_3, \end{aligned}$$

where all the $\alpha^{(m)}_{i,s,r}, \beta^{(m)}_{i,s}, \gamma^{(m)}_{i,s}$ are functions of ζ and η. The solution for the linearized partial differential equations (27)-(29) is obtained by approximating the exact solutions of $f(\eta,\zeta)$, $\theta(\eta,\zeta)$ and $\phi(\eta,\zeta)$ by the Lagrange form of polynomial $F(\eta,\zeta)$, $\Theta(\eta,\zeta)$ and $\Phi(\eta,\zeta)$ at the selected collocation points; $0 = \zeta_0 < \zeta_1 < \zeta_2 < \cdots < \zeta_{N_\zeta} = 1$. The approximation for $f(\eta,\zeta)$ and $\theta(\eta,\zeta)$ has the form

$$\begin{aligned} f(\eta,\zeta) &\approx \sum_{j=0}^{N_\zeta} F(\eta,\zeta)L_j(\zeta) \\ &= \sum_{j=0}^{N_\zeta} F_j(\eta)L_j(\zeta), \end{aligned} \tag{30}$$
$$\begin{aligned} \theta(\eta,\zeta) &\approx \sum_{j=0}^{N_\zeta} \Theta(\eta,\zeta)L_j(\zeta) \\ &= \sum_{j=0}^{N_\zeta} \Theta_j(\eta)L_j(\zeta), \end{aligned} \tag{31}$$
$$\begin{aligned} \phi(\eta,\zeta) &\approx \sum_{j=0}^{N_\zeta} \Phi(\eta,\zeta)L_j(\xi) \\ &= \sum_{j=0}^{N_\zeta} \Phi_j(\eta)L_j(\zeta). \end{aligned} \tag{32}$$

where $F_j(\eta) = F(\eta,\zeta)$, $\Theta_j(\eta) = \Theta(\eta,\zeta)$ and $\Phi_j(\eta) = \Phi(\eta,\zeta)$, L_j is the characteristic Lagrange cardinal polynomial defined as

$$L_j(\zeta) = \prod_{k=0,k\neq j}^{M} \frac{\zeta-\zeta_k}{\zeta_j-\zeta_k}, \tag{33}$$

that obey the Kronecker delta equation

$$L_j(\zeta_k) = \Delta_{jk} = \begin{cases} 0 & \text{if} \quad j \neq k \\ 1 & \text{if} \quad j = k \end{cases} \tag{34}$$

The equations for the solution of $F_j(\eta)$, $\Theta_j(\eta)$ and $\Phi_j(\eta)$ are obtained by substituting (30)-(32) into (27)-(29) and letting the equations be satisfied at the points $\zeta_i, i = 0,1,2,\ldots,N_\zeta$. The derivatives of the Lagrange polynomial can be computed analytically with the transformation $\zeta \in [0, L_\zeta]$ to $\omega \in [-1,1]$ then we consider the Chebyshev-Gauss-Lobatto points $\omega_i = \cos\frac{i\pi}{N_\zeta}$. After using linear transformation $\zeta = L_\zeta(\omega+1)/2$, the derivatives of f' with respect to the collocation points ω_j is computed as

$$\left.\frac{\partial f'}{\partial\zeta}\right|_{\zeta=\zeta_i} = 2\sum_{j=0}^{N_\zeta} F'_j(\eta)\frac{dL_j}{d\zeta}(\zeta_i) = \sum_{j=0}^{N_\zeta} \mathbf{d}_{i,j}F'_j(\eta),$$
$$i = 0,1,2,\ldots,N_\zeta, \tag{35}$$

where $\mathbf{d}_{i,j} = \frac{dL_j}{d\omega}(\omega_i)(i = 0,1,\ldots,N_\zeta)$ are entries of the standard Chebyshev differentiation matrix,

$\mathbf{d} = \frac{2}{L_\zeta} d$. We now apply the collocation (η, ζ_i) in (27)-(29) we obtain

$$\mathbf{A}_{1,1}^{(i)}\mathbf{F}_{1,i}^{(i)} + \mathbf{A}_{1,2}^{(i)}\mathbf{F}_{2,i}^{(i)} + \mathbf{A}_{1,3}^{(i)}\mathbf{F}_{3,i}^{(i)} + \beta_{1,r}^{(i)} \sum_{j=0}^{N_\zeta} \mathbf{d}_{i,j}\mathbf{F}_{i,j} + \gamma_{1,r}^{(i)} \sum_{j=0}^{N_\zeta} \mathbf{d}_{i,j}\mathbf{D}\,\mathbf{F}_{i,j} = R_{1,j}, \quad (36)$$

$$\mathbf{A}_{2,1}^{(i)}\mathbf{F}_{2,i}^{(i)} + \beta_{2,r}^{(i)} \sum_{j=0}^{N_\zeta} \mathbf{d}_{i,j}\mathbf{F}_{2,i} = R_{2,j}, \quad (37)$$

$$\mathbf{A}_{3,1}^{(i)}\mathbf{F}_{3,i}^{(i)} + \beta_{3,r}^{(i)} \sum_{j=0}^{N_\zeta} \mathbf{d}_{i,j}\mathbf{F}_{3,i} = R_{3,j}, \quad (38)$$

where

$$\mathbf{A}_{1,1}^{(i)} = \sum_{s=0}^{3} \alpha_{1,s,r}\mathbf{D}^{(s)}, \mathbf{A}_{1,2}^{(i)} = \sum_{s=0}^{3} \alpha_{2,s,r}\mathbf{D}^{(s)},$$
$$\mathbf{A}_{1,3}^{(i)} = \sum_{s=0}^{3} \alpha_{3,s,r}\mathbf{D}^{(s)}\mathbf{A}_{2,1}^{(i)} = \sum_{s=0}^{3} \alpha_{2,s,r}^{(2)}\mathbf{D}^{(s)},$$
$$\mathbf{A}_{3,1}^{(i)} = \sum_{s=0}^{3} \alpha_{3,s,r}^{(3)}\mathbf{D}^{(s)}.$$

3.2 Bivariate Local Linearization Method

The systematic way of implementing the local linearization method is given as

$$\sum_{v=0}^{p}\left[\beta_{v,r}^{(1)}\frac{\partial f_{v,r+1}}{\partial\zeta} + \gamma_{v,r}^{(1)}\frac{\partial f'_{v,r+1}}{\partial\zeta}\right] + \sum_{s=0}^{p}\alpha_{1,s,r}^{(1)} f_{1,r+1}^{(s)} = R_1, \quad (39)$$

$$\sum_{v=0}^{p}\left[\beta_{v,r}^{(2)}\frac{\partial f_{v,r+1}}{\partial\zeta} + \gamma_{v,r}^{(2)}\frac{\partial f'_{v,r+1}}{\partial\zeta}\right] + \sum_{s=0}^{p}\alpha_{2,s,r}^{(2)} f_{2,r+1}^{(s)} = R_2, \quad (40)$$

$$\vdots$$

$$\sum_{v=0}^{p}\left[\beta_{v,r}^{(n)}\frac{\partial f_{v,r+1}}{\partial\zeta} + \gamma_{v,r}^{(n)}\frac{\partial f'_{v,r+1}}{\partial\zeta}\right] + \sum_{s=0}^{p}\alpha_{n,s,r}^{(n)} f_{n,r+1}^{(s)} = R_n, \quad (41)$$

where

$$R_1 = \sum_{v=0}^{p}\left[\beta_{v,r}^{(1)}\frac{\partial f_{v,r}}{\partial\zeta} + \gamma_{v,r}^{(1)}\frac{\partial f'_{v,r}}{\partial\zeta}\right] + \sum_{s=0}^{p}\alpha_{1,s,r}^{(1)} f_{1,r}^{(s)} - \Gamma_1, \quad (42)$$

$$R_2 = \sum_{v=0}^{p}\left[\beta_{v,r}^{(2)}\frac{\partial f_{v,r}}{\partial\zeta} + \gamma_{v,r}^{(2)}\frac{\partial f'_{v,r}}{\partial\zeta}\right] + \sum_{s=0}^{p}\alpha_{2,s,r}^{(2)} f_{1,r}^{(s)} - \Gamma_2, \quad (43)$$

$$\vdots$$

$$R_n = \sum_{v=0}^{p}\left[\beta_{v,r}^{(n)}\frac{\partial f_{v,r}}{\partial\zeta} + \gamma_{v,r}^{(n)}\frac{\partial f'_{v,r}}{\partial\zeta}\right] + \sum_{s=0}^{p}\alpha_{n,s,r}^{(n)} f_{1,r}^{(s)} - \Gamma_n. \quad (44)$$

Applying the local linearization method to (24)-(26) we obtain the following

$$\alpha_{1,0,r}^{(1)} f_{1,r+1} + \alpha_{1,1,r}^{(1)} f'_{1,r+1} + \alpha_{1,2,r}^{(1)} f''_{1,r+1} + \alpha_{1,3,r}^{(1)} f'''_{1,r+1} + \beta_{0,r}^{(1)}\frac{\partial f_{1,r+1}}{\partial\zeta} + \gamma_{1,r}^{(1)}\frac{\partial f'_{1,r+1}}{\partial\zeta} = R_1, \quad (45)$$

$$\alpha_{2,0,r}^{(2)} f_{2,r+1} + \alpha_{2,1,r}^{(2)} f'_{2,r+1} + \alpha_{2,2,r}^{(2)} f''_{2,r+1} + \beta_{0,r}^{(2)}\frac{\partial f_{2,r+1}}{\partial\zeta} = R_2, \quad (46)$$

$$\alpha_{3,0,r}^{(3)} f_{3,r+1} + \alpha_{3,1,r}^{(3)} f'_{3,r+1} + \alpha_{3,2,r}^{(3)} f''_{3,r+1} + \beta_{0,r}^{(3)}\frac{\partial f_{3,r+1}}{\partial\zeta} = R_3. \quad (47)$$

where

$$\alpha_{1,0,r}^{(1)} = \frac{1}{2} f''_r, \alpha_{1,1,r}^{(1)} = -\zeta\frac{\partial f'_r}{\partial\zeta},$$
$$\alpha_{1,2,r}^{(1)} = \frac{1}{2} f_r + \zeta\frac{\partial f_r}{\partial\zeta},\ \alpha_{1,3,r}^{(1)} = \left(1 + \frac{1}{\delta}\right),$$
$$\beta_{0,r}^{(1)} = \zeta f''_r,\ \gamma_{1,r}^{(1)} = -\zeta f'_r,$$
$$R_1 = \alpha_{1,0,r}^{(1)} f_{1,r} + \alpha_{1,1,r}^{(1)} f'_{1,r} + \alpha_{1,2,r}^{(1)} f''_{1,r} + \alpha_{1,3,r}^{(1)} f'''_{1,r} + \beta_{0,r}^{(1)}\frac{\partial f_{1,r}}{\partial\zeta} + \gamma_{1,r}^{(1)}\frac{\partial f'_{1,r}}{\partial\zeta} - \Gamma_1,$$

$$\alpha_{2,0,r}^{(2)} = 0,\ \alpha_{2,1,r}^{(2)} = \frac{1}{2}f_r + \zeta\frac{\partial f_r}{\partial \zeta} + \epsilon_1 f_r'',$$
$$\alpha_{2,2,r}^{(2)} = \frac{1}{Pr}\left(1 + \frac{4}{3}R\right) + \epsilon_1 f_r',\ \beta_{0,r}^{(2)} = -\zeta f_r',$$
$$R_2 = \alpha_{2,0,r}^{(2)} f_{2,r} + \alpha_{2,1,r}^{(2)} f_{2,r}' + \alpha_{2,2,r}^{(2)} f_{2,r}'' + \beta_{0,r}^{(2)}\frac{\partial f_{2,r}}{\partial \zeta} - \Gamma_2,$$

$$\alpha_{3,0,r}^{(3)} = 0,\ \alpha_{3,1,r}^{(3)} = \frac{1}{2}f_r + \zeta\frac{\partial f_r}{\partial \zeta} + \epsilon_2 f_r'',$$
$$\alpha_{3,2,r}^{(3)} = \frac{1}{Sc} + \epsilon_2 f_r',\ \beta_{0,r}^{(3)} = -\zeta f_r'$$
$$R_3 = \alpha_{3,0,r}^{(3)} f_{3,r} + \alpha_{3,1,r}^{(3)} f_{3,r}' + \alpha_{3,2,r}^{(3)} f_{3,r}'' + \beta_{0,r}^{(3)}\frac{\partial f_{3,r}}{\partial \zeta} - \Gamma_3.$$

where all the $\alpha_{i,s,r}^{(m)}, \beta_{i,s}^{(m)}, \gamma_{i,s}^{(m)}$ are functions of ζ and η. The full description of the application of the Chebyshev spectral collocation technique is fully described in [23].

4 Results and discussions

The problem of the effect of convective boundary conditions, viscous heating and double dispersion in Casson fluid flow was solved by the local linearization (BLLM). The system of equations was validated by the quasi-linearization method for the case $\zeta = 0$ which gives a well-known Blasius equation and compared to the results of Yih [25]. These comparisons of results were in excellent agreement. In this section we focus on the variation of the Casson parameter δ, thermal convection parameter λ, double diffusion parameter N, radiation parameter R, thermal stratification parameter ϵ_1, Eckert number Ec, stratification parameter ϵ_2, Soret number Sr and the Biot number Bi concentration, temperature and velocity profiles. We also study variation of some selected physical parameters with the skin friction, mass and heat transfer coefficients.

In this section we assume that the Prandtl number is between $Pr = 10$ at 20^oC and $Pr = 20$ for blood. All other parameters are chosen arbitrarily being careful to stay within the range of the Casson fluid non- Newtonian parameters.

We discuss the accuracy of the BLLM by considering the residual error after r iterations over $i = 0, 1, \ldots, N_t$. The method converges with the computational order of convergence rate (COC=1).

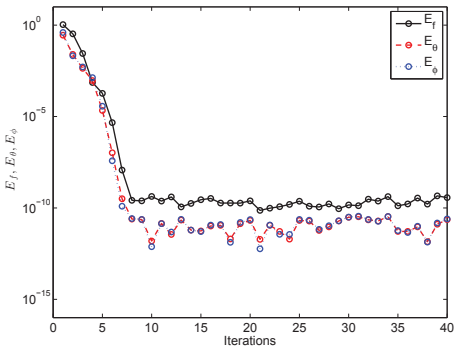

Figure 1: Error for $f(\eta), \theta(\eta), \phi(\eta)$

Figure 1 shows the error approximated at a given iteration level as $E_f = ||f_{r+1} - f_r||_\infty, E_\theta = ||\theta_{r+1} - \theta_r||_\infty, E_\phi = ||\phi_{r+1} - \phi_r||_\infty$. The method converges after five iterations and becomes stable until 40 iterations showing the accuracy of the BLLM. The residual error is $O(10^{-13})$ for $\theta(\eta)$ and $\phi(\eta)$ and 10^{-10} for $f(\eta)$. The errors incurred are as a result of interpolation and ill conditioned matrices. The variation of certain parameters results in changing the condition number of large matrices.

The numerical results were validated for the skin friction $f''(0)$ and heat transfer $-\theta'(0)$ coefficients for the Newtonian fluid. The results obtained by the BLLM and the quasi-linearization method were compared to the results obtained by Yih [25] and were in excellent agreement as shown in Table 1 and Table 2.

Table 1: Comparison of the values of $f''(0)$ and $-\theta'(0)$ of Yih et al. [25] with QLM when $\zeta = R = Ec = 1/\delta = \epsilon_1 = \epsilon_2 = 0$.

	ref [25]		QLM	
Pr	$f''(0)$	$-\theta'(0)$	$f''(0)$	$-\theta'(0)$
1	0.332057	0.332057	0.33205935	0.33205935
10	-	-	0.3305935	0.72814593

Table 2: Comparison of the values of $f''(0)$, $-\theta'(0)$ of Yih et al. [25]and QLM (see Table 1) with BLLM when $\zeta = R = Ec = 1/\delta = \epsilon_1 = \epsilon_2 = 0$.

	ref [25]		BLLM	
Pr	$f''(0)$	$-\theta'(0)$	$f''(0)$	$-\theta'(0)$
1	0.332057	0.332057	0.33205935	0.33205935
10	-	-	0.3305935	0.72814593

In this section a set of graphical results for the temperature,velocity and concentration profiles as well as the local heat and mass transfer coefficients are presented and discussed. Detailed solutions have

been obtained and are presented in figures 2-12. The numerical problem consist of two variables (ζ, η) and three dependent fluid dynamics variables (f, θ, ϕ). In the computations in this paper default parameters are prescribed as $\delta = 1, \lambda = 0.05, N = 0.5, Pr = 10, R = 0.5, Ec = 0.1, \epsilon_1 = 0.1, \epsilon_2 = 0.1, Sc = 0.7, Sr = 0.1, Bi = 0$.

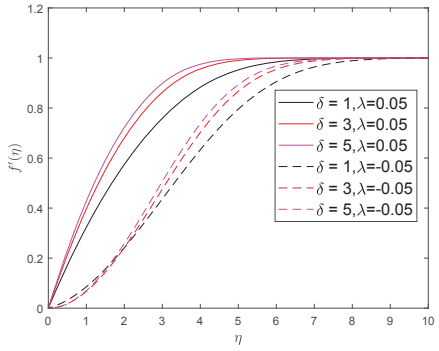

Figure 2: Effects of varying Casson parameter δ on velocity profiles

Figure 2 is plotted to examine the effects of varying the Casson parameter on velocity profiles $f'(\eta)$ when $\delta = 1, 3, 5$. Increasing the non-Newtonian Casson parameter result in the increase in the velocity profiles in both aiding $(\lambda = 0.05)$ and opposing flows $(\lambda = -0.05)$. Larger values of the non-Newtonian parameter implies that fluid becomes Newtonian $(\frac{1}{\delta} \rightarrow 0)$, thereby increasing the boundary layer fluid velocity.

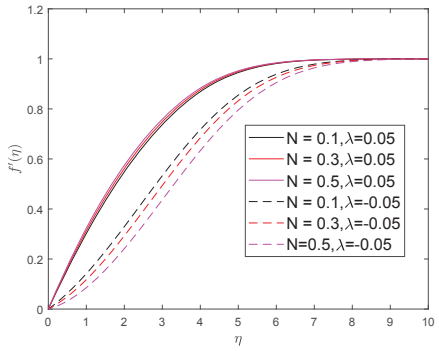

Figure 3: Effects of varying double diffusion parameter N on velocity profiles

Figure3 is plotted to examine the effects of varying the double diffusion parameter on velocity profiles $f'(\eta)$ when $N = 0.1, 0.3, 0.5$. Increasing the double diffusion parameter causes the increase in velocity profiles in both aiding $(\lambda = 0.05)$ and opposing flows $(\lambda = -0.05)$. Increasing the double diffusion parameter means that solutal convection is more enhanced than thermal convection. The concentration gradient is more enhanced than the temperature gradient. This effect result in the increase in velocity profiles.

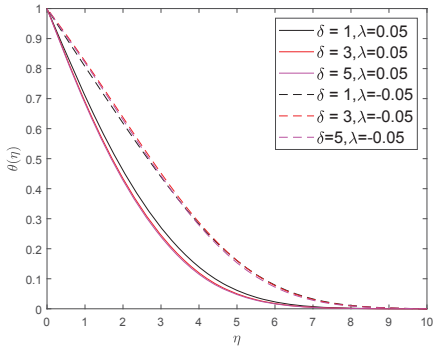

Figure 4: Effect of varying Casson parameter δ on temperature profiles

Figure 4 is plotted to examine the effects of varying the Casson parameter on temperature trends $\theta(\eta)$ when $\delta = 1, 3, 5$ for both assisting $\lambda = 0.05$ and opposing flow $\lambda = -0.05$. Increasing the Casson parameter result in the lowering in temperature trends. Larger values of the Casson parameter imply high velocities in the boundary layer enhancing heat transfer. Opposing flow enhance temperature trends,similar results were reported in Ramachandra et al.[2].

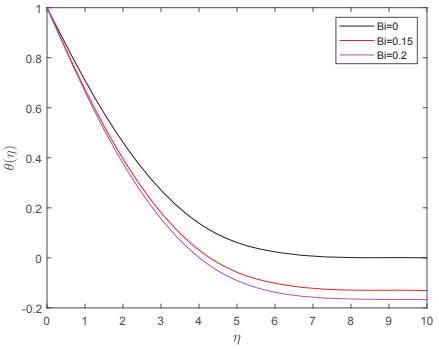

Figure 5: Effect of varying Biot number Bi on temperature profiles

Figure 5 is plotted to examine the effects of varying the Biot number Bi on temperature profiles $\theta(\eta)$ when $Bi = 0, 0.15, 0.2$. Increasing the Biot number result in the decrease in the temperature pro-

files. Here we note that the values of the Biot numbers are less than 1; this is because of the uniformity of the temperature inside the vertical surface. The Biot number measures the heat transfer resistance in the solid boundary. It is noted from the graph that the heat transfer coefficient decreases with increasing Biot number.

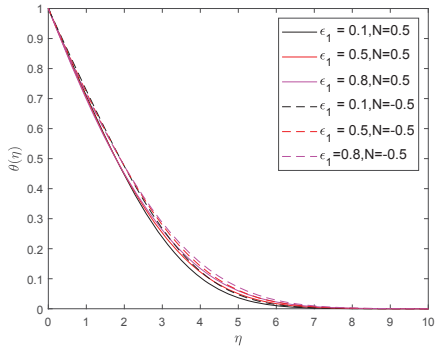

Figure 6: Effects of thermal stratification parameter ϵ_1 on temperature profiles

Figure 6 is plotted to examine the effects of thermal stratification parameter ϵ_1 on temperature trends $\theta(\eta)$ when $\epsilon_1 = 0.1, 0.5, 0.8$. Increasing the ϵ_1 result in the decrease in temperature profiles. The ambient conditions considered in this study are not constant but varies. Increasing the thermal stratification parameter decrease the temperature gradient thereby reducing heat transfer. The reverse effect noted is caused by the increase in temperature further away from the vertical surface.

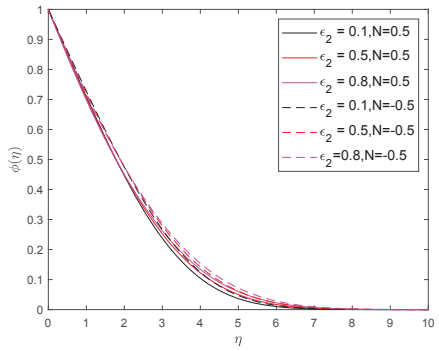

Figure 7: Effects of solutal stratification parameter ϵ_2 on the concentration profiles

Figure 7 depict the effect of varying solutal stratification parameter ϵ_2 on concentration trends profiles $\phi(\eta)$ when $\epsilon_2 = 0.1, 0.5, 0.8$. Increasing the ϵ_2 result in the decrease in concentration profiles. The ambient solute conditions change with distance away from the vertical plate. Increasing the solutal stratification parameter decrease the concentration gradient thereby reducing mass transfer. The reverse effect noted is as a result of the increase in solute further away from the vertical surface.

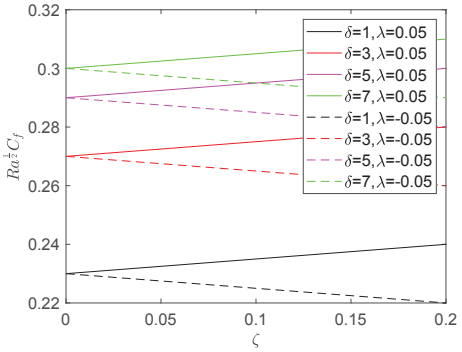

Figure 8: Plot of the skin friction coefficient $f''(0)$ against transverse coordinate ζ for different values of the Casson parameter δ

Figure 8 depicts the plot of skin friction coefficient $f''(0)$ against the transverse coordinate ζ for different values of the Casson parameter δ for both aiding and opposing thermal convection. From the graph is noted that increasing the Casson parameter β would cause the drop in the skin friction coefficient. The increase in the Casson parameter would cause the reduction of the shear stress on the vertical surface thereby reducing skin friction coefficient. The skin friction coefficient increases with increasing ξ for the aiding case $(\lambda = 0.05)$ and decreases with increasing ξ for the opposing case $(\lambda = -0.05)$.

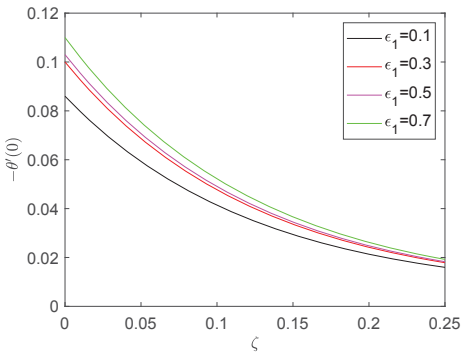

Figure 9: Effects of varying thermal stratification parameter ϵ_1 on heat transfer coefficient $-\theta'(0)$

In Figure 9, the graph of the heat transfer number

against the transverse coordinate for various values of the thermal stratification parameter ϵ_1 is shown. Increasing the thermal stratification parameter result in the decrease in the heat transfer number. The increase in the stratification parameter has an effect of reducing the temperature gradient thereby reducing the heat transport from the surface of the vertical wall. The heat transfer number values fall with increasing ζ.

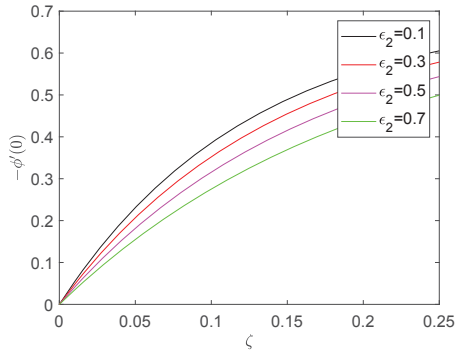

Figure 10: Effects of varying solutal stratification parameter ϵ_2 on the mass transfer coefficient $-\phi'(0)$

In Figure 10 depicts the plot of the mass transfer coefficient against the transverse coordinate for different values of the solutal stratification parameter ϵ_2. Increasing the solutal stratification parameter result in the decrease in the mass transfer coefficient. The increase in the solutal stratification parameter would have an effect of reducing the concentration gradient thereby reducing the mass transfer coefficient. The mass transfer coefficient increase with increasing ζ.

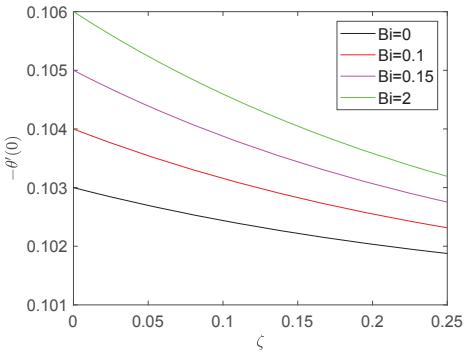

Figure 11: Effects of varying Biot number Bi on heat transfer coefficient $-\theta'(0)$

In Figure 11, it noted that increasing the Biot number result in the decrease in the heat transfer coefficient. Increasing the Biot number has an effect of increasing the heat flow resistance in the solid boundary thereby reducing heat transfer into the fluid.

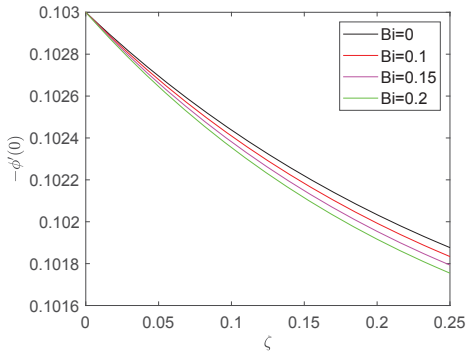

Figure 12: Effects of varying Biot number Bi on mass transfer coefficient $\phi'(0)$

In Figure 12 it is also noted that increasing the Biot number result in the increase in mass transfer coefficient. The mass transfer coefficient decrease with increasing transverse coordinate ζ.

5 Conclusion

The effect of the double dispersion in convection of Casson fluid flow along a vertical plate have been studied. In this study we used the bivariate local linearization method (BLLM) to solve the governing system of equations. The accuracy of the method was compared to previous studies in the literature. The BLLM converge linearly after five iterations and becomes stable up 20 iterations showing the accuracy of this method. The results were also in excellent agreement with those of the quasi-linearization method for the case $\zeta = 0$ as shown in Tables 1 and 2. The new contribution of this work is the implementation of the BLLM in solving partial differential equations in fluid flow which yields more accurate results and is easy to use. The new and previously reported numerical computations have shown that; Increasing both the Casson parameter δ and double diffusion parameter N, increase the velocity profiles in both aiding and opposing flow. Increasing both the Casson parameter δ and Biot number Bi reduce temperature profiles. Increasing the thermal stratification parameter ϵ_1 decrease the temperature profiles, and increasing the solutal stratification parameter ϵ_2 also decreases the concentration profiles. Increasing the Casson parameter δ would have an effect of increasing the skin friction coefficient in both aiding and opposing cases. Increasing the thermal stratification parameter ϵ_1 and the solutal stratification parameter ϵ_2 would have an effect of reducing both the heat transfer coefficient $-\theta'(0)$ and the mass transfer coefficient $-\phi'(0)$ respectively. Increasing the Biot number Bi would have an effect of reducing both heat and mass transfer coefficients respectively. These results concur with some of those that are reported in the literature confirming that the

numerical method used can be considered as an alternative method in solving boundary value problems.

Acknowledgements: The research was supported by the Faculty Research and Innovation Committee (FRIC) of the Central University of Technology, Free Sate in South Africa.

References :

[1] Awad, F. G., Sibanda, P., Motsa, S. S., Makinde, O. D, Convection from an inverted cone in porous medium with cross diffusion, Computers with Mathematics Applications, 2011:61: 1431-1441.

[2] Ramachandra, P. V., Sua, R. A., Anwar, B. O, Flow and heat transfer of Casson fluid from a horizontal circular cylinder with partial slip in non-Darcy porous medium, Applied and Computational Mathematics, 2013:2: 1-12.

[3] Narayana, P. A. L, Murthy, P.V.S.N., Free convective heat and mass transfer in a doubly stratified non-Darcy porous medium, Transactions of the ASME - Journal of Heat Transfer, 2006:128: 1204-1212.

[4] Kairi, R. R, Murthy, P.V.S.N., Free convection in a thermally stratified non-Darcy porous medium, International Journal of Fluid Mechanics Res., 2009:36:414-423.

[5] Srinivasacharya, D., RamReddy, Ch, Effect of double stratification on free convection in a micropolar fluid, Transactions of the ASME - Journal of Heat Transfer, 2011:133: 122502 (7 Pages)

[6] Murthy, P.V.S.N., RamReddy, Ch., Chamkha, A. J, Rashad, A. M, Magnetic effect on thermally stratified nanofluid saturated non-Darcy porous medium under convective boundary condition, International Communication in Heat and Mass Transfer, 2013:47: 41-48.

[7] Kameswaran, P. K., Sibanda, P., Thermal dispersion effects on convective heat and mass transfer in an Ostwald de Waele nanofluid flow in porous media, Boundary Value Problems (2013) 2013:243. https://doi.org/10.1186/1687-2770-2013: 243

[8] Chen, C.H., Combined heat and mass transfer in MHD free convection from a vertical surface with Ohmic heating and viscous dissipation, International Journal of Engineering Science, 2004:42: 699-713.

[9] Narayana, P. A. L., Gorla, R.S.R., Sibanda, P., Soret and Dufour effects on free convection along a vertical wavy surface in a fluid saturated Darcy porous medium, International Journal of Heat and Mass Transfer, 2010:53:3030-3034.

[10] Javaherdah, K., Nejad, M. M., Moslemi, M., Natural convection heat and mass transfer in MHD fluid flow past a moving vertical plate with variable surface temperature and concentration in a porous medium, Engineering Science and Technology, an International Journal, 2015:18: 423-431.

[11] Raju, M. C., Varma, S. V. K., Seshaiah, B., Heat transfer effects on viscous dissipative fluid flow past a vertical plate in the presence of induced magnetic field, Ain Shams Engineering Journal, 2015:6333-339.

[12] Casson, N., A flow equation for pigment-oil suspensions of the printing ink type. In: Mill, C.C. (ed.), Rheology of Disperse System, Pergamon Press, Newyork, Oxford, 1959:84-104.

[13] Vinogradov, G. V., Malkin, A. Y, Rheology of polymers, Mir Publisher, Moscow, 1979.

[14] McDonald, D. A, Blood flows in Arteries, 2nd Edition, Chap. 2., Arnold, London, 1974.

[15] Shaw, S., Gorla, R.S.R., Murthy, P.V.S.N., Ng, C. O, Pulsatile Casson fluid flow through a stenosed bifurcated artery, International Journal of Fluid Mechanics Research, 2009:36: 43-63.

[16] Mukhopaddhyay, S., De, P. R., Bhattacharyya, K., Layek, G. C., Casson fluid flow over an unsteady stretching surface, Ain Shams Engineering Journal, 2013:4: 933-938.

[17] Mukhopaddhyay, S., Vajravelu, K., Diffusion of chemically reactive species in Casson fluid flow over an unsteady permeale stretching surface, Journal of Hydrodynamics, 2013:25: 591-598.

[18] Nadeem, S., Ul Haq, R., Akbar, N. S., Khan, Z. H., MHD three-dimensional Casson fluid flow past a porous linearly stretching sheet, Alexandria Engineering Journal, 2013:52:577-582.

[19] Zueco, J., Network simulation method applied to radiation and dissipation effects on MHD unsteady free convection over vertical porous plate, Applied Mathematical Modelling, 2007:31: 2019-2033.

[20] Suneetha, S., Bhaskar R. N., Ramachandra P. V., Radiation and mass transfer effects on MHD free convection flow past an impulsively started isothermal vertical plate with dissipation,Thermal Science, 2009:13: 71-181.

[21] Kameswaran, P. K., Narayana, M., Sibanda, P., Murthy, P., Hydromagnetic nanofluid flow due to a stretching or shrinking sheet with viscous dissipation and chemical reaction effects, International Journal of Heat and Mass Transfer, 2012:55: 7587-7595.

[22] Nakamura, M., Sawada, T., Numerical study on the flow of a non-Newtonian fluid through an asymmetric stenosis, Journal of Biomechanical Engineering, 1988:110:137-143.

[23] Motsa, S. S., Magagula, V. M, Sibanda, P., A bivariate Chebyshev spectral collocation quasilinearization method for nonlinear evolution parabolic equations,The Scientific World Journal, 2014:doi: 10.1155/2014/581987

[24] Bellman, R. E, Kalaba, R. E, Quasilinearization and nonlinear boundary value problems, 1965,Elsevier, New York

[25] Yih,K. A Blowing/suction effect on combined convection in stagnation flow over a vertical plate embedded in porous medium, Chinese J. Mech. A, 1999i:15:41-45